Chapter 13
Gaussian Scale Concept to Reduce the Computation in Detection of Surface Defects in Machine Vision

P. Satheesh, B. Srinivas, and P. Rama Santosh Naidu

Introduction

Visual examination using artificial intelligence and machine learning approaches is increasingly popular over the years for assessing surface flows of manufactured products and materials [1]. Techniques of visual examination are shown to deliver quick statistical evaluations with enhanced performance and productivity at a cheap cost [2].

Turbines are enormous machining cylinders used to fire shells and are mounted massive howitzers. As the bullet explodes and glides into the turbines, temperature and pressure build-up, gradually degrading the surface [3]. The deteriorated surface imperfections may cause the projectile to launch incorrectly, or possibly endanger the lives of those controlling it. As a result, assessing flaws in damaged turbines is critical [4].

On worn turbines, the main kinds of flaws recognized are ordinary wearing, corrosive pits, erosion, and rusting. The development of wearing is due the relative velocity of the projectile and also gun barrel. Destructive pitting and degradation is caused by the impact of combustion [5]. The oxidization of the surface causes rusting. If the damaged region exceeds a certain threshold, the turbines would be repaired or discarded. As a result, the flaws must be discovered, categorized, and also by the region assessed [6]. In this case, mechanical approaches are challenging because

P. Satheesh (✉) · B. Srinivas · P. Rama Santosh Naidu
MVGR College of Engineering, Vizianagaram, India
e-mail: satish@mvgrce.edu.in

B. Srinivas
e-mail: srinio.b@mvgrce.edu.in

P. Rama Santosh Naidu
e-mail: prsnaidu@mvgrce.edu.in

Ch. Satyanarayana et al. (eds.), *Proceedings of the International Conference on Computer Vision, High Performance Computing, Smart Devices and Networks*, Advanced Technologies and Societal Change,
https://doi.org/10.1007/978-981-19-4044-6_14

they are slow, inconsistent, and prone to human mistakes. The form and length of the turbines also makes bare-eye examination difficult [7–9].

Related Works

The goal of this research is to develop a foundation for detecting and classifying flaws on the surfaces of turbines to use a machine learning technique. In recent times, the visual surface examination is performed on a wide range of items, including front seals and PU packaging. Several fault detections, segmentation solutions are proposed and performed successfully.

Depending on the requirements, there seem to be a variety of characteristics to be picked. It is discovered that characteristics based on texture descriptions produced superior outcomes. Techniques for automatically selecting characteristics are not frequently employed. Features extraction strategies are used by a community of scholars. There seem to be numerous classifications accessible to identify faults [10]. Many researchers [11] found that the Support Vector Machine (SVM) used to have a high degree of accuracy. Some researchers have discovered Artificial Neural Network (ANN) efficiently to be satisfactory for this kind of purpose. It has been noted that limited study on categorizing faults on the surfaces of turbines is published. This research proposes and implements a methodology for recognizing and categorizing surface structure in the turbine at the laboratory scale. Surfaces images showing the damaged areas of 10 utilized turbines are taken using a Charge Coupled Device (CCD) sensor and a small microscope probing in a non-destructive method. The first step is to classify the problems into three groups: typical wearing, no-defect, and also the remainder of the faults. The flaws are again divided and also faulty regions determined to use the expanded maximum transformation. For categorization, many textural characteristics depending on histogram and GLCM are retrieved from the segmentation images. Different classifications like Bayes, k-NN, ANN, and SVM are used to test the remaining flaws. All of these processes are performed at various levels, with the optimum scale selected based on segmented and higher accuracy. The computing effectiveness of the whole inspection process is ensured by Gaussian scaled separation approach.

Proposed Works

The inner surface image capture of the utilized cylinders is done with a CCD camera and a small optical coupler. Figure 13.1 shows a schematic representation of the experimental set-up utilized for images acquired. The lighting is provided by an LED that would be dispersed by a reflected ray. The light's course is depicted in the schematic image [12]. The camera, which is coupled to an optical probing and illuminated, maybe rotated horizontally and vertically within the turbine to take

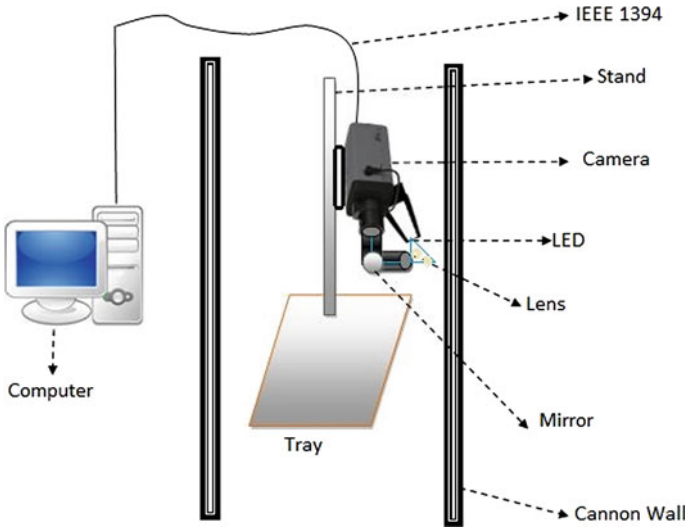

Fig. 13.1 Schematic diagram of the experimental set-up

photos of the whole inside area. The device is calibrated by recording the image of an optic grating with a resolution of 1/100 mm and calculating the pixel that correspond to it.

A total of 1000 images is chosen from a massive pool of images collected from the inner side of 10 utilized turbines at specific segments, with 200 images per class, including such eroding, corrosive pits, generally, corrosion, and also no. Figure 13.2 depicts the 5 types of faults. Cross-validation uses half of the photos from every category to evaluate the accuracy of segments and classification. Depending on the actual truth, the square of the exposed surfaces in metric measurements is estimated and validated for correctness. By physically segregating the images utilizing Adobe Photoshop CS5 program and turning the faulty pixel to red and also the remainder pixel to blues, the high accuracy of the imperfection is produced. MATLAB is used to award 1 and 0 to defective and non-defective squares, accordingly, depending on the manual choice of colors.

Results and Discussions

To use the forward's feature selection algorithm, a few essential parts for categorization are selected automatically from the image characteristics. Several classifiers, including Mahalanobis distance matrix classifiers, Euclidean minimum distance classification algorithm, Naive Bayes-Nearest Neighbor (k-NN), Artificial Neural Network (ANN), and SVM Classifiers, are trained using the relevant attributes acquired via selecting features (SVM). The clustering algorithm for each of them is

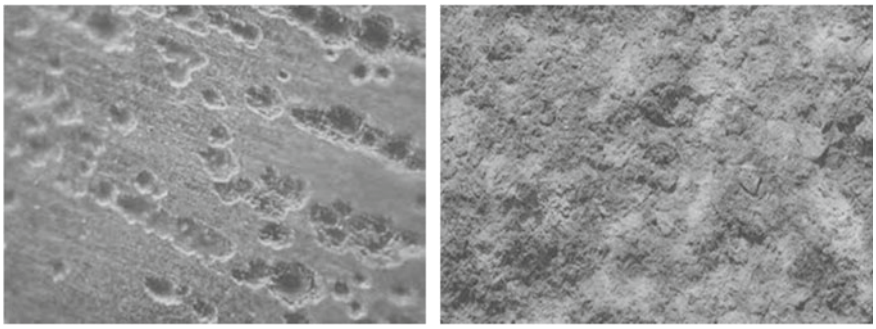

(a) Pitting (b) Rust

Fig. 13.2 Dataset's categories

used to evaluate their accuracy. A flow diagram depicting the steps taken to finish the process categorization is presented in Fig. 13.3. All these operations are performed out on six different image numerical strengths, with the optimal scaling being chosen depending on segment and accuracy rate. This spatial pyramid idea is developed to ensure that the research' computing effectiveness never is compromised at the expense of efficiency.

The information is classified into three groups for the classification step, including 200 images representing regular wear, 200 images representing no defect, and 600 images representing the other three types of errors. Half of every class is allocated for programs of study. Cross-validation is used to divide the training and certification in 50% of the time. From every scale, two characteristics are derived for the classification step: average gray level and sample variance. After using the Otsu method

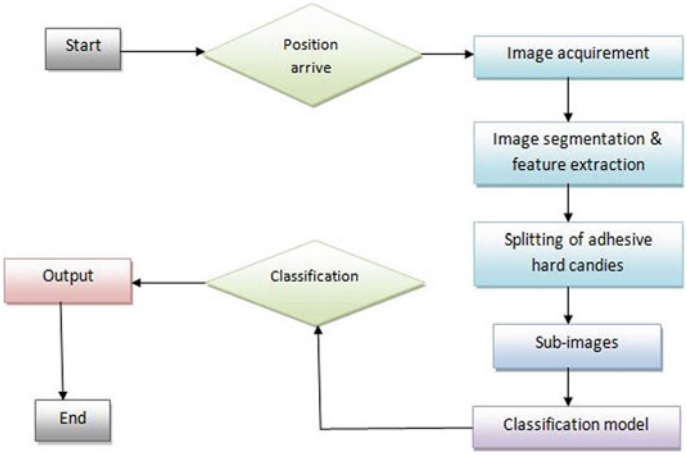

Fig. 13.3 Process of actual fault

Table 13.1 Classification

	Others	No-defect	Normal wear
Others	597	0	5
No-defect	0	200	0
Normal Wear	5	0	197
Accuracy = 99.3%			

to global threshold the photos, the average gray value is determined. Because of its high brightness in any of those photos, the average gray level of typical wearing is considered lower than some other problems. Due to the obvious homogeneity in gray levels, the standard error for images without any defects would be lower. For every level, Mahalanobis and Euclidean minimal similarity classifier is a learning guide depending on these characteristics. Both classifications exhibit nearly comparable levels of accuracy.

The Euclidean minimum distance learner is chosen because it takes less time to compute than the Distance measure classifier, which requires the creation of a covariance matrix. Table 13.1 shows the prediction model for the first classification employed in this study. Following the initial categorization, the photos having typical wearing are enhanced to make the fault appear darker throughout all types of faults. Several adaptive threshold approaches are investigated, including Otsu, area dividing, watershed transformation, and expanded maxima convert.

To reduce sounds, morphology treatments including image erosion and dilation are used following classification. The correctness of the split area is checked against the previously determined underlying data. For every fault class, Table 13.2 lists the procedures and their reliability. Figure 13.4 presents a comparison of several segment findings for a typical wear image. Including all types of flaws, the expanded maximum transformation is found to provide reasonable performance.

The correctness of the testing data is assessed using Bayes, k-Nearest Neighbor, Artificial Neural Network, and Support Vector Machine classifications. For Bayes, the previous likelihood is considered to be the same for all categories. In the k-NN approach, the number of clusters is adjusted, and also the best k is determined to be 5 depending on assessment efficiency. The variance in assessment and learning efficiency as the number of clusters increases is seen in Fig. 13.5a. For ANN, the number of layers varies, and three hidden levels are chosen for term accuracy. Figure 13.5b shows the change in efficiency as a function of the number of hidden nodes.

The categorization is completed at all scale-space regions. Figure 13.6 shows the changes in reliability for classification phase, segment, and end categorization using

Table 13.2 Various segmentation techniques

Method	Accuracy (%)
Otsu	56
Region based	66
Watershed	82
Extended maxima	87

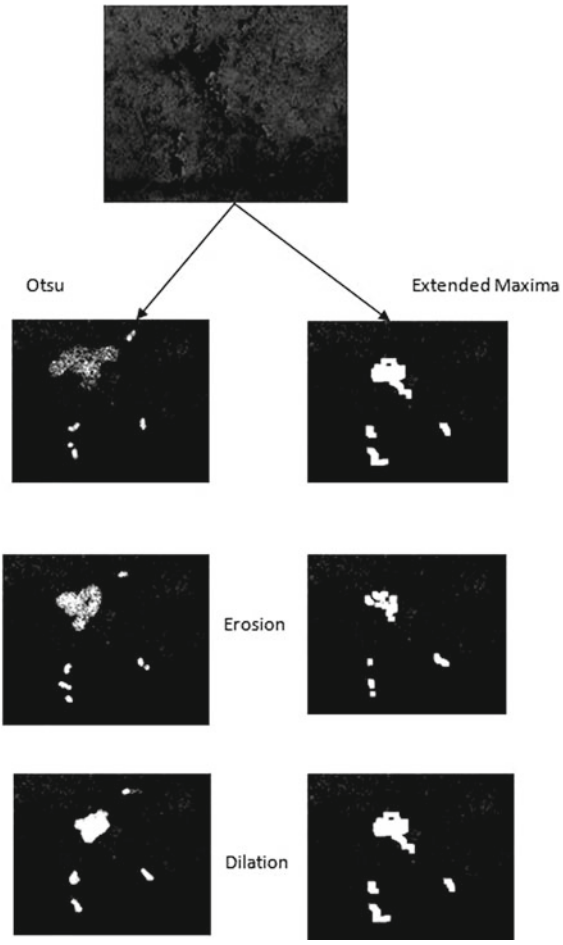

Fig. 13.4 Feature extraction using proposed system

varied scale-spaces of images. The reliability of the initialization step, segmented, and end classification techniques are seen to be preserved until the Gaussian pyramid scaling grade of 3 is reached. The use of scaling separation in pattern categorization showed to be useful in terms of computational power.

The highest image testing period is 0.7 s, a 20% decrease in duration due to lower scalability, and hence it may be used in live time for automated processes.

Conclusion

Surfaces flaws of the used turbine are identified and classified using artificial intelligence and machine learning approaches. Surface area images of a turbine having

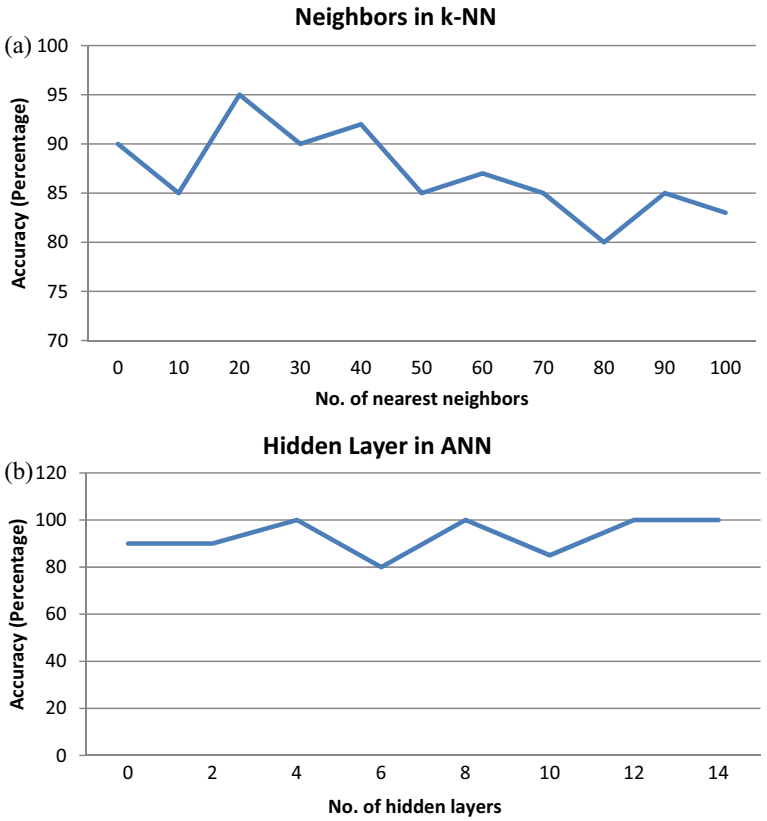

Fig. 13.5 Various classifiers using KNN and ANN

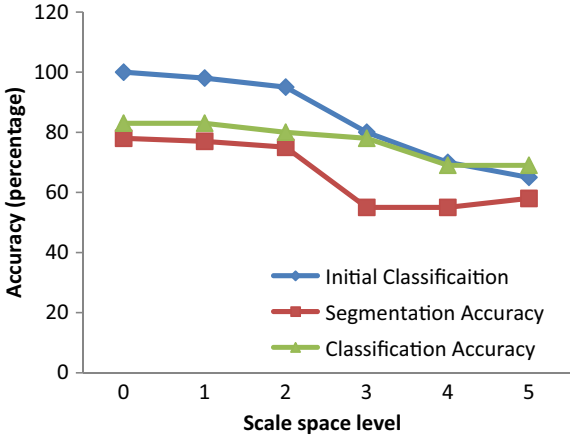

Fig. 13.6 Comparison of proposed and existing system

surface cracks are taken, identified, and saved in a database. Natural wear, erosion, corrosive pitting, corrosion, and no-defect are the five types of allocation. Every image type is created as a multiresolution Gaussian pyramid. Unlike other faults, the flaws become larger in normal wear. As a result, an initial classification is carried out to determine the reason for segmentation. The standard error and average gray level are used as characteristics. For this initialization step, the Euclidean distance measure predictor scored well in terms of effectiveness and processing time. Among the various segmentation techniques employed, the extended-maxima transformation worked well. The size of every flaw is quantified metric measurements to use an optic grating to calibrate the sensor. The extracted features yielded 12 texture factors based on the distribution and GLCM. For the classification purpose, five characteristics are chosen to use a progressive forwards feature selection algorithm. Including an efficiency of 96.67%, SVM appears as the top predictor among the various classifications evaluated. The six-level, multi-level Gaussian gradient is developed for computational detection and segmentation of flaws while keeping the same rate of precision. This is found to be well into the image space using grade 3.

References

1. Zhang, W., Tan, A., Zhou, G., Chen, A., Li, M., Chen, X., Hu, Y., et al.: A method for classifying citrus surface defects based on machine vision. J. Food Meas. Charact. **15**(3), 2877–2888 (2021)
2. Sampath, V., Maurtua, I., Aguilar Martín, J.J., Gutierrez, A.: A survey on generative adversarial networks for imbalance problems in computer vision tasks. J. Big Data **8**(1), 1–59 (2021)
3. Gupta, K.K., Mukhopadhyay, T., Roy, A., Roy, L., Dey, S.: Sparse machine learning assisted deep computational insights on the mechanical properties of graphene with intrinsic defects and doping. J. Phys. Chem. Solids **155**, 110111 (2021)
4. Xu, C., Zhu, G.: Intelligent manufacturing lie group machine learning: real-time and efficient inspection system based on fog computing. J. Intell. Manuf. **32**(1), 237–249 (2021)
5. Stephen, O., Maduh, U.J., Sain, M.: A machine learning method for detection of surface defects on ceramic tiles using convolutional neural networks. Electronics **11**(1), 55 (2021)
6. Dong, C.Z., Catbas, F.N.: A review of computer vision-based structural health monitoring at local and global levels. Struct. Health Monit. **20**(2), 692–743 (2021)
7. Benbarrad, T., Salhaoui, M., Kenitar, S.B., Arioua, M.: Intelligent machine vision model for defective product inspection based on machine learning. J. Sens. Actuator Netw. **10**(1), 7 (2021)
8. Chen, L., Yao, X., Xu, P., Moon, S.K., Bi, G.: Rapid surface defect identification for additive manufacturing with in-situ point cloud processing and machine learning. Virtual Phys. Prototyping **16**(1), 50–67 (2021)
9. Yasuda, T., Ookawara, S., Yoshikawa, S., Matsumoto, H.: Machine learning and data-driven characterization framework for porous materials: permeability prediction and channeling defect detection. Chem. Eng. J. **420**, 130069 (2021)
10. Latchoumi, T.P., Parthiban, L.: Quasi oppositional dragonfly algorithm for load balancing in cloud computing environment. Wirel. Pers. Commun. 1–18 (2021)
11. Hu, W., Wang, W., Ai, C., Wang, J., Wang, W., Meng, X., Qiu, S., et al.: Machine vision-based surface cracks analysis for transportation infrastructure. Autom. Constr. **132**, 103973 (2021)
12. Voronin, V., Sizyakin, R., Zhdanova, M., Semenishchev, E., Bezuglov, D., Zelemskii, A.: Automated visual inspection of fabric images using a deep learning approach for defect detection. In: Automated Visual Inspection and Machine Vision IV, vol. 11787, p. 117870P. International Society for Optics and Photonics (2021, June)